JOURNAL OF MATERIALS SCIENCE 14 (1979) 1339–1343

Thermal conversion efficiency of an ideal thermoelastic marmem cycle

H. A. MOHAMED
Energy and Environment Division, Lawrence Berkeley Laboratory, University of California, Berkeley, California 94720, USA

The thermal conversion efficiency of an ideal stress–strain–temperature cycle based on the mechanical shape memory effect associated with a thermoelastic martensite transformation (thermoelastic marmem* cycle) has been studied. A relationship between the upper limit of the thermal efficiency and a set of materials properties has been derived. It is shown that a higher thermoelastic marmem efficiency and a closer approach to the corresponding Carnot efficiency are favoured by: (1) higher yield stress of the high-temperature phase, (2) larger recoverable strain, (3) smaller transformation temperature range and thermal hysteresis associated with the transformation, and (4) smaller transformation latent heat. The thermal efficiency has been calculated for a cycle utilizing a Ti–50.4 at % Ni alloy. The highest efficiency for this particular alloy was found to be about 9%; this amounts to 45% of the corresponding Carnot efficiency. Thus it is concluded that efficiencies can be obtained which are comparable with those of cycles operating at small temperature differences with fluids as working media.

1. Introduction

The mechanical shape memory effect exhibited by a large number of alloys is a phenomenon associated with thermoelastic martensite transformations [1]. A demonstration of the memory effect involves:

(a) inducing a permanent strain within a certain range at a lower temperature where the martensite phase is thermodynamically stable, followed by

(b) heating across the martensite → high-temperature phase transformation temperature range.

During heating and as the martensite reverts to the high-temperature phase, the strain is recovered. Complete strain recovery is achieved when the reversion of martensite is completed. Thus, the martensite transformation has an important effect on the stress–strain–temperature behaviour of the material. This is shown schematically in Fig. 1. The stress, σ_1, required to induce a strain, ϵ, within the recoverable range at a lower temperature where the martensite phase is thermodynamically stable in the absence of stress, is much smaller than the corresponding stress, σ_2, at a higher temperature where the martensite phase is stable only in the presence of stress. The stress build-up during heating ($\sigma_2 - \sigma_1$ in Fig. 1) is referred to as the recovery stress and is defined as the stress required to counterbalance the driving

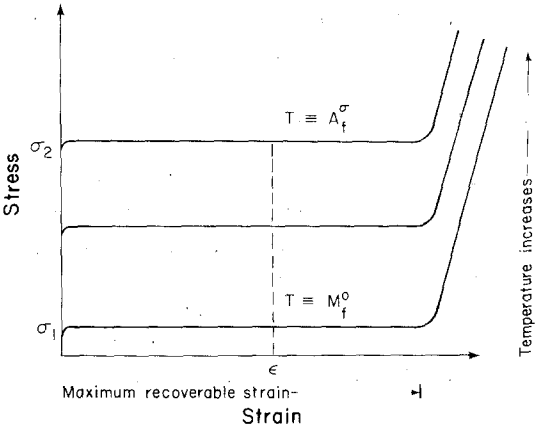

Figure 1 Typical tensile stress–strain diagrams of a shape memory alloy at different temperatures within the temperature range $M_f^0 - A_f^\sigma$.

*Marmem is derived from martensite memory [21].

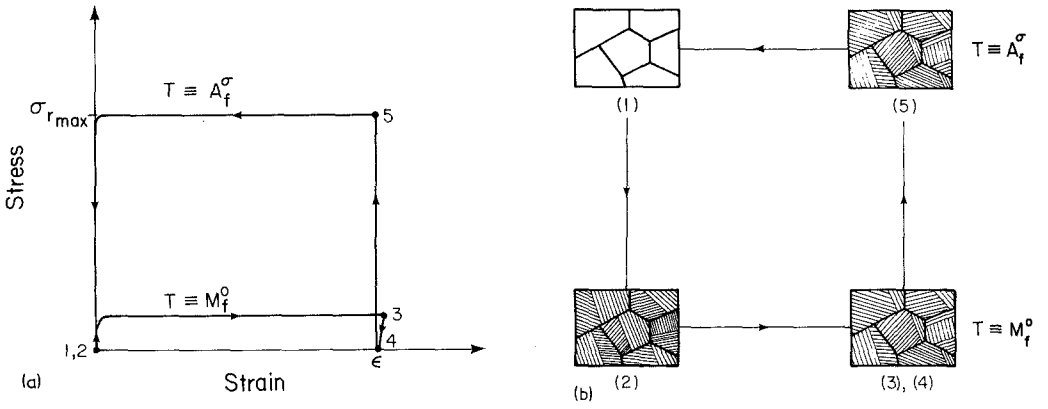

Figure 2 (a) Ideal stress–strain–temperature cycle in two dimensions. (b) Schematic illustration of the microstructural changes which occur during the cycle of (a); (1) high-temperature phase at A_f^σ temperature in the absence of an external stress; (2) thermal martensite at the M_f^0 temperature; (3, 4) deformed martensite at the M_f^0 temperature; (5) deformed martensite at the A_f^σ temperature in the presence of an external stress $\sigma_{r,\,max}$.

force of the martensite → high-temperature phase transformation. This stress–strain–temperature behaviour can thus be considered to be due to:

(1) reversibility of the deformation modes that accomodate the strain within the recoverable range [2–4], and

(2) increasing the thermodynamic instability of the martensite phase as the temperature increases within the range $A_s - A_f^*$.

Therefore, in principle, a shape memory alloy can be made to perform the function of converting heat into useful mechanical work by subjecting it to an appropriate stress–strain–temperature cycle in a solid-state heat engine. Recently, versions of solid-state heat engines comprising shape memory alloys as working media have been demonstrated [5–7]. Owing to the relatively small transformation temperature range (tens of degrees), such heat engines may prove to be important in converting low temperature, large-heat sources such as solar energy. The competitive applicability of a shape memory alloy in a solid-state heat engine can be measured by:

(1) thermal efficiency,

(2) work output per mass unit, this partially determines the power output, and

(3) fatigue life.

Recently, attempts have been made to calculate the thermal efficiency of a particular stress–strain–temperature cycle [8, 10]. In these calculations, the work output was regarded as being the work done by an arbitrary constant force during heating, and the results were inconclusive. In the present investigation, the thermal efficiency of an ideal cycle has been examined with reference to the recovery stresses generated by the material during heating.

2. Ideal thermoelastic marmem cycle

The path of an ideal thermoelastic marmem cycle that gives the maximum work output for a given recoverable strain is shown schematically on the stress–strain plot of Fig. 2a. The microstructural changes which occur during the entire cycle are illustrated in Fig. 2b. The path of the cycle consists of two isotherms, 234 and 51, and two isochores, 45 and 12 (an isochoric process is one during which no external work is exchanged between the system and its surroundings). The working medium is a polycrystalline shape memory alloy.

2.1. Temperature difference across the cycle

The cycle is assumed to operate between the temperatures A_f^σ and M_f^0. It is assumed that upon cooling to the M_f^0 temperature, all the crystallographically equivalent martensite variants form with equal probability. Therefore, in the absence of an external stress, the material does not acquire

*A_s and A_f are the temperatures at which the reversion of martensite to the high-temperature phase starts and finishes, respectively, during heating. M_s and M_f are the temperatures at which the transformation to martensite starts and finishes, respectively, during cooling. In the absence of an external stress, these temperatures will be given the superscript 0, and in the presence of an external stress they will be given the superscript σ.

a net macroscopic strain relative to the point where it consists entirely of the high-temperature phase at the A_f^σ temperature.

Thus, the lower temperature of the cycle is fixed by the M_f^0 temperature. It has been shown theoretically [11] and experimentally [1] that the transformation temperatures increase linearly with increasing stress; therefore,

$$A_f^\sigma = A_f^0 + C\sigma \ldots \quad (1)$$

where C is a constant and σ is an external stress. In the discussions which follow, we assume that a heat sink exists at the M_f^0 temperature and a heat sources(s) exists at the appropriate A_f^σ temperature.

2.2. Procedure of the cycle

Referring to Fig. 2, the cycle consists of the following steps:

$1 \rightarrow 2$ The material is cooled from the A_f^σ to the M_f^0 temperature to transform it almost entirely to martensite in the absence of an external stress.

$2 \rightarrow 4$ A strain ϵ (excluding the normal elastic strain) within the recoverable range is induced by applying an external stress σ_1 and then the stress is released at the M_f^0 temperature.

$4 \rightarrow 5$ The material is heated to the A_f^σ temperature while entirely constraining the strain ϵ. This requires a continuously increasing external stress, σ_r, to counterbalance the driving force of the martensite $\rightarrow$ high-temperature phase transformation (the driving force arises from the free energy difference between the martensite and high-temperature phase). Recently, it has been shown that σ_r achieves its maximum value at the A_f^σ temperature and that this maxiumum can be expressed as [12]:

$$\sigma_{r,max} = \sigma_y^{htp} [1 - \exp^{-N\epsilon}] \quad (2)$$

where σ_y^{htp} is the yield stress of the high-temperature phase and N is the number of crystallographically equivalent martensite variants that exist prior to straining.

$5 \rightarrow 1$ At the A_f^σ temperature, the external stress, $\sigma_{r,max}$, is infinitesimally decreased. Therefore, the driving force of the transformation overcomes the external stress and thus the martensite reverts to the high-temperature phase and the strain ϵ is recovered. During this process, work, W, is done on the surroundings and latent heat of the transformation, ΔH, is absorbed. As the transformation to the high-temperature phase and strain recovery are completed, the external stress, $\sigma_{r,max}$ ($\sigma_{r,max} < \sigma_y^{htp}$) is released and the material becomes ready to repeat the cycle.

3. Thermal conversion efficiency

Referring to Fig. 2a, the maximum useful work, W, per unit volume per cycle, can be expressed as:

$$W = \sigma_y^{htp}(1 - \exp^{-N\epsilon}) \cdot \epsilon. \quad (3)$$

Thus, a higher work output is favoured by a higher yield stress of the high-temperature phase and a higher recoverable strain. The total heat absorbed by the material during the entire cycle, ΔQ, is given by

$$\Delta Q = \Delta H + \bar{C}p\,[A_f^\sigma - M_f^0]$$

where $\bar{C}p$ is the average specific heat of the material over the temperature range $A_f^\sigma - M_f^0$.

This can be rewritten as:

$$\Delta Q = \Delta H + \bar{C}p\,[(A_f^0 - A_s^0) + (A_s^0 - M_f^0) + C\sigma_y^{htp}(1 - \exp^{-N\epsilon})], \quad (4)$$

$(A_f^0 - A_s^0)$ is the transformation temperature range in the absence of an external stress and $(A_s^0 - M_f^0)$ is a measure of the thermal hysteresis associated with the transformation.

The thermal efficiency η_{th} can thus be written as

$$\eta_{th} = \frac{\sigma_y^{htp}(1 - \exp^{-N\epsilon}) \cdot \epsilon}{\Delta H + \bar{C}p\,[(A_f^0 - A_s^0) + (A_s^0 - M_f^0) + C\sigma_y^{htp}(1 - \exp^{-N\epsilon})]} \quad (5)$$

The corresponding Carnot efficiency, η_c, is given by:

$$\eta_c = 1 - \frac{M_f^0}{A_f^\sigma}. \quad (6)$$

It can be concluded from Equations 5 and 6 that a higher thermoelastic marmem efficiency and a closer approach to the corresponding Carnot efficiency are expected to be favoured by:

(1) higher yield stress of the high-temperature phase,

(2) larger recoverable strain,

(3) smaller transformation temperature range and thermal hysteresis associated with the transformation, and

(4) smaller latent heat.

Fig. 3 shows schematically a desirable thermal hysteresis loop (a) versus an undesirable one (b).

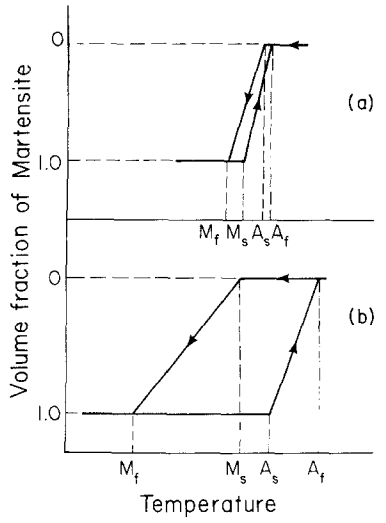

Figure 3 Thermal hysteresis loops associated with the martensite transformation; loop (a) favours higher thermoelastic marmem efficiency than loop (b).

4. Application to a Ti–50.4 at % Ni alloy

Some of the properties which determine the thermal efficiency as depicted from Equation 5 have been measured for a Ti–50.4 at % Ni alloy. The specimens in the form of wires, 0.5 mm diameter, have been annealed at 600° C for 24 h in a vacuum furnace (about 10^{-5} mm Hg) and then furnace-cooled to room temperature.

The transformation temperatures and their functional dependence on stress have been measured using a specially designed laser-beam dilatometer. It has been observed that the transformation temperatures during cooling and heating increase linearly with increasing stress at about the same rate. The transition entropy, ΔS, has been calculated from the rate of change of the transformation temperatures with stress and a modified Clausius–Clapeyron equation. The latent heat of the transformation at the equilibrium temperature (T_0) has been calculated from $T_0 \Delta S$. The equilibrium transition temperature, T_0, has been approximately determined from [13]

$$T_0 = M_s^0 + \tfrac{1}{2}\,[A_s^0 - M_f^0].$$

The yield stress of the high temperature phase and the recoverable strain range have been determined from tensile stress–strain data. The yield stress of the high-temperature phase has been observed to be nearly independent of temperature within the temperature range of interest. A similar result has been reported for other Ni–Ti alloys [14]. This is consistent with the relatively high melting point of Ni–Ti alloys near the equiatomic composition (about 1300° C [15]). The results of these measurements are summarized in Table I.

TABLE I

Transformation temperatures (° C)	M_s^0 24	M_f^0 5	A_s^0 26	A_f^0 33	T_0 35
$C \equiv dA_f/d\sigma$, ° C (kg mm^{-2})$^{-1}$		1.14			
Transition entropy, ΔS (cal/g.-atom/deg)		1.0			
latent heat, ΔH at 35° C (cal/g.-atom)		308*			
σ_y^{htp} (kg mm^{-2})		42.0			
Maximum recoverable strain (%)		8			

*For a Ti–51 at. % Ni alloy a value of 307 cal/g.-atom at 40° C was reported [22]. 1 g.-atom = 53.3 g.

The number of crystallographically equivalent martensite variants, N, has been taken to be 24. This number follows from the crystallographic theory of the martensite transformation in an Au–47.5 at. % Cd alloy [16]. The crystallographic features of the transformation in Ni–Ti alloys have been observed to be very similar to those in a Au–47.5 at. % Cd alloy [17, 18].

The average specific heat has been taken to be 5 cal/g. atom/deg. from the available experimental data [18]. In the calculation of the thermal efficiency, it has been assumed that the latent heat of the transformation is independent of temperature. This assumption is justified in view of the observed negligible change in specific heat upon the transformation [18].

Thus, the highest efficiency for the cycle of Fig. 2 and the particular alloy considered has been calculated using Equation 5, and the data of Table I. This has been found to be about 9% (the work output is 4.3 J gm^{-1}) for $A_f^\sigma = 74°$ C and $M_f^0 = 5°$ C. The corresponding Carnot efficiency is 20%. Therefore, the thermoelastic marmem efficiency amounts to 45% of the corresponding Carnot efficiency. This result is comparable with those of cycles operating at comparable temperature differences with fluids as working media [19, 20].

It is expected that, with selecting or designing shape memory alloys that have better combinations of properties, higher efficiencies can be obtained. Furthermore, it is expected that solid-state heat engines with shape memory alloys as working media are rather simple, since they do not require boilers and heat exchangers; they are also environmentally acceptable. It should be noted,

however, that the fatigue strength may limit the amount of strain that the material can sustain for millions of cycles without failure, although deformation by motion of twin boundaries [2] is expected to result in an extended fatigue life.

5. Conclusions

The thermal conversion efficiency of an ideal thermoelastic marmem cycle based on the mechanical shape memory effect associated with thermoelastic martensite transformations has been studied. A relationship between the efficiency and a set of materials properties has been derived. It is shown that a higher efficiency and a closer approach to the corresponding Carnot efficiency are favoured by:

(1) higher yield stress of the high-temperature phase,

(2) larger recoverable strain,

(3) smaller transformation temperature range and thermal hysteresis associated with the transformation, and

(4) smaller transformation latent heat.

The efficiency has been calculated for a Ti–50.4 at. % Ni alloy and it is concluded that efficiencies can be obtained (9%) which are comparable with those of cycles operating at small temperature differences with fluids as working media.

Acknowledgements

The technical assistance of Mr R. Banks and Mr W. Hubert in obtaining the experimental data is greatly appreciated. This work was supported by the Conservation and Solar Applications Division of the US Department of Energy through the Energy and Environment Division of the Lawrence Berkeley Laboratory, University of California, Berkeley.

References

1. J. PERKINS, editor, "Shape Memory Effects in Alloys" (Plenum Press, New York, 1975).
2. H. A. MOHAMED and J. WASHBURN, *J. Mater. Sci.* **12** (1977) 469.
3. C. M. WAYMAN, in "Shape Memory Effects in Alloys" (Plenum Press, New York, 1975) p. 1.
4. L. DELAEY, R. V. KRISHNAN, H. TAS and H. WARLIMONT, *J. Mater. Sci.* **9** (1974) 1521.
5. B. CUNNINGHAM and K. H. G. ASHBEE, *Acta Met.* **25** (1977) 1315.
6. R. BANKS and M. WAHLIG, Presented at the International Solar Energy Society Meeting, Winnepeg, Canada, August 1976; Lawrence Berkeley Laboratory Report LBL-5293.
7. R. BANKS, in "Shape Memory Effects in Alloys" (Plenum Press, New York, 1975) p. 537.
8. A. A. GOLESTANEH, *J. Appl. Phys.* **49** (1978) 1241.
9. H. C. TONG and C. M. WAYMAN, *Met. Trans.* **6A** (1975) 29.
10. M. AHLERS, *Scripta Met.* **8** (1975) 71.
11. H. C. TONG and C. M. WAYMAN, *ibid* **8** (1974) 93.
12. H. A, MOHAMED, *J. Mater. Sci.* **13** (1978) 2728.
13. *Idem, ibid* **13** (1978) 1364.
14. W. B. CROSS, A. H. KARIGITS and F. J. STIMLER, "Nitinol Characterization Study", NASA Contractor Report (1969) Cr-1433.
15. C. M. JACKSON, H. J. WAGNER and R. J. WASILEWSKI, "55-Nitinol – The Alloy with a Memory: Its Physical Metallurgy, Properties, and Applications", NASA Report (1972) SP 5110.
16. D. S. LIEBERMAN, M. S. WECHSLER and T. A. READ, *J. Appl. Phys.* **26** (1955) 473.
17. H. A. MOHAMED, Ph. D. Thesis, University of California, Berkeley (1976), Lawrence Berkeley Laboratory Report LBL-5112.
18. S. P. GUPTA and A. A. JOHNSON, *Trans. Jap. Inst. Metals* **14** (1973) 292.
19. D. PRIGMORE and R. BARBER, *Solar Energy* **17** (1975) 185.
20. H. TABOR and L. BRONICKI, "Small Turbine for Solar Power Package" in Proceedings of the United Nations Conference on New Sources of Energy", Vol. 4 (Solar Energy: 1) (United Nations Publications, 1964) p. 68.
21. C. M. WAYMAN and K. SHIMIZU, *Met. Sci. J.* **6** (1972) 175.
22. I. E. WANG, W. T. BUEHLERAND and P. J. PICKERT, *J. Appl. Phys.* **36** (1965) 3232.

Received 31 July and accepted 25 September 1978.